MODELLING RESIDUAL STRAINS DURING THE CYCLING OF TI-NI AND TI-NI-CU SHAPE MEMORY ALLOYS UNDER PSEUDOELASTICITY CONDITIONS

Strnadel, B., Kursa, M.
VŠB - Technical University of Ostrava, Faculty of Metallurgy and Materials Engineering, 17. listopadu 15, 708 33 Ostrava, Czech Republic; bohumir.strnadel@vsb.cz, miroslav.kursa@vsb.cz,

MODEL REZIDUÁLNÍ DEFORMACE BĚHEM CYKLOVÁNÍ TI-NI A TI-NI-CU SLITIN S TVAROVOU PAMĚTÍ V PSEUDOELASTICKÉM STAVU

Strnadel, B., Kursa, M.
VŠB – TU Ostrava, Fakulta Metalurgie a materiálového inženýrství, 17. listopadu 15, 708 33 Ostrava, Česká republika; bohumir.strnadel@vsb.cz, miroslav.kursa@vsb.cz

Abstrakt

V příspěvku je studována odezva tří typů Ti-Ni a tří typů Ti-Ni-Cu slitin s tvarovou pamětí v pseudoelastickém stavu na mechanické cyklování při tvrdém a měkkém cyklickém zatěžování. Experimentální výsledky potvrdily, že reziduální deformace po odtížení s rostoucím počtem cyklů roste, zatímco kritické napětí pro indukci martenzitu a energie disipovaná během jednoho cyklu s rostoucím počtem cyklů klesá. Vyšší hodnota kritického napětí pro skluz a intenzivnější cyklické dislokační zpevnění podporované vyšší maximální deformací a vyšším aplikovaným napětím redukuje obecně rychlost při které zbytková deformace s rostoucím počtem cyklů vzrůstá a to má za následek stabilizaci cyklické napěťově deformační křivky. Nízká hodnota kritického skluzového napětí ve slitinách s nízkým obsahem niklu a stejně tak cyklické deformační zpevnění vyvolává větší vnitřní pnutí a rychlejší pokles kritického napětí nutného pro vznik martenzitické transformace během cyklování. Skutečnost, že hystereze s rostoucím počtem cyklů klesá je důsledkem omezení transformační deformace, která je způsobena při tvrdém cyklování kumulací zbytkové deformace a při měkkém cyklování hlavně vzrůstem rezistence dislokační struktury proti pohybu fázových hranic. Nižší hodnoty niklu ve slitině vykazují nižší skluzové napětí a větší zbytkovou plastickou deformaci, proto hystereze u těchto slitin klesá silněji při měkkém než při tvrdém cyklování. Na základě podrobné analýzy šíření plastické deformace ve vzorku podrobeném cyklickému zatěžování byl zpracován model závislosti reziduálního prodloužení na počtu cyklů. Tento model umožňuje definovat tři hlavní faktory, které kontrolují hodnotu zbytkového prodloužení v závislosti na počtu cyklů. Prvním z nich je zbytková plastická deformace způsobená dislokačním zpevněním po tepelném zpracování slitiny, dalšími dvěma parametry souvisejí s cyklickým deformačním zpevněním a popisují jak zbytková deformace roste s rostoucím počtem cyklů a jak naopak klesá, když kritické skluzové napětí roste. Model dává velmi dobrou shodu s experimentálními výsledky a lze jej účelně využít při designu konstrukčních částí mechatronických robotických systémů.

Abstract

The effect of three types Ti-Ni shape memory alloys in pseudoelasticity state on mechanical cycling has been studied under conditions of hard and soft loading cycling. Experimental results proved that the residual deformation after unloading increases with increasing number of cycles, however the critical stress for the induction of martensite and the

energy dissipated in one cycle decline in the course cycling. A higher critical stress for slip, and more intense cyclic dislocation hardening promoted by greater maximum deformation and greater maximum applied stresses, in general reduce the rate at which residual elongation grows with the number of cycles, and tend to stabilize the cyclic stress-elongation diagrams. The small magnitude of critical stress for slip in low nickel alloys, as well as cyclic strain hardening induce greater internal stresses and a more marked decrease of the critical stress for the induction of martensite as cycling progresses. The fact that hysteresis diminishes in the course of cycling is due to the restriction of transformation strain, which is caused in hard cycling by the cumulation of residual strain and in soft cycling chiefly by the increasing resistance of the dislocation structure against movements of the phase boundary. Lower nickel alloys display lesser slip stresses and more residual plastic strain, and therefore their hysteresis drops off more rapidly in hard than in soft cycling. Detailed analysis of plastic deformation propagation in cyclically loaded specimen helped to work out a model of the dependence of residual elongation on the number of cycles. This model enables to identify the three main factors that govern the magnitude of the residual elongation. One is the residual plastic elongation caused by dislocation hardening after the alloy is heat treated, and the other two are cyclic strain hardening parameters describing how residual elongation grows with the number of cycles, and how this residual elongation is reduced, as cycles increase, by the rising critical stress level for slip. The model has proved to yield very close agreement with experimental findings. This results can be employed as a design tool of structural parts in mechatronics and robotics systems.

Keywords: shape memory alloys; Ti-Ni alloy; Ti-Ni-Cu alloy; pseudoelasticity; critical stress for inducing martensite; plastic strain propagation; mechanical cycling.

1. Introduction

Pseudoelasticity occurs in shape memory alloys, such as Ti-Ni and Ti-Ni-Cu alloys, above the austenite finish temperature A_f. This state allows a number of interesting technical applications of these alloys in such fields as robotics, medicine, or nuclear engineering. However, a prerequisite of most such applications is stability of the fundamental pseudoelasticity characteristics in the course of mechanical cycling. The residual elongation e_0 after the load is relieved, the critical stress σ_{ms} for the induction of martensite, and the hysteresis W (or energy dissipated in one cycle) have to remain stable during cycling, else the components made of such alloys could not be expected to function reliably in service.

Experimental research into the responses of Ti-Ni and Ti-Ni-Cu alloys to mechanical cycling [1-4] has proved that their stress-strain behavior is not only temperature dependent, but also strongly dependent on the nickel content, the heat treatment, and the loading mode. For most practical applications, the stability of the cyclic stress-strain diagrams is best judged by the way residual strain varies with the number of cycles. The experiments mentioned above have demonstrated that residual strain after unloading, sometimes judged by the residual specimen elongation, grows with the number of cycles because of an accumulation of plastic strain. This finding has been explained qualitatively, chiefly with regard to the nickel contents; but so far no quantitative model has been evolved to describe adequately how residual strain alters in the course of cycling. The work reviewed in the present paper was aimed at compiling such a model, and confronting its results with experimental findings made in the mechanical cycling of Ti-Ni and Ti-Ni-Cu alloys at a constant temperature in the pseudoelastic domain. Again, the stability

of the stress-strain characteristics will necessarily have to be examined with reference to the nickel contents.

2. Experimental details and results

The investigated materials were three Ti-Ni alloys with slightly different but roughly equiatomic compositions, and three Ti-Ni-Cu alloys containing 10 at. % Cu at the expense of their Ni contents. These alloys, summarized in Table 1, were produced in an induction furnace with an argon atmosphere. Plate tensile specimens were prepared from cold rolled strips. The specimens, shown in Fig.1, were polished with emery glass paper, then vacuum annealed for 1 hour at 400°C and water quenched to ensure the most effective dislocation hardening and hence a maximum increase of the critical stress for slip. The martensite finish and start temperatures, M_f and M_s, as well as the austenite start and finish temperatures A_s and A_f, were ascertained by differential scanning calorimetry, and are listed along with the chemical compositions in Table 1.

Table 1 Alloy compositions and transformation temperatures

Alloy	Composition, at. %			Transformation points, °C			
	Ti	Ni	Cu	M_f	M_s	A_s	A_f
A	49.1	50.9	-	-115.8	-30.7	1.9	44.6
B	49.5	50.5	-	-77.8	-18.5	9.0	53.0
C	50.0	50.0	-	-28.0	37.5	48.2	77.8
D	49.0	41.0	10.0	7.6	29.8	34.5	50.0
E	50.0	40.0	10.0	20.9	41.4	52.7	66.6
F	48.5	41.5	10.0	14.4	37.5	42.6	60.6

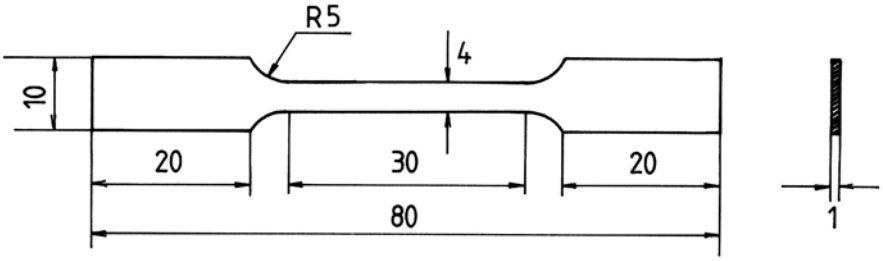

Fig.1 Shape and size of the specimens

Mechanical cycling was performed on a computer controlled precision universal tester, with a heating chamber, at a constant 80°C, a temperature at which all these alloys were in a pseudoelastic state (see Table 1 and the results in [4]). Two different cycling modes were employed: one specimen of each alloy was subjected to 50 cycles in the tensile region with a maximum elongation e_{max} of 1 mm, which is known as hard cycling; another specimen of each alloy underwent 50 soft cycles where the maximum

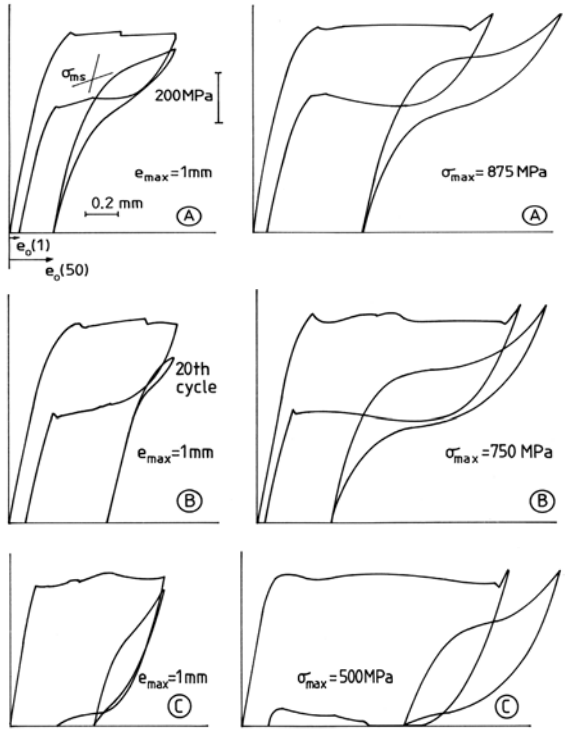

Fig.2a Stress-strain characteristics after the first and fiftieth cycles of binary Ti-Ni alloys A, B and C

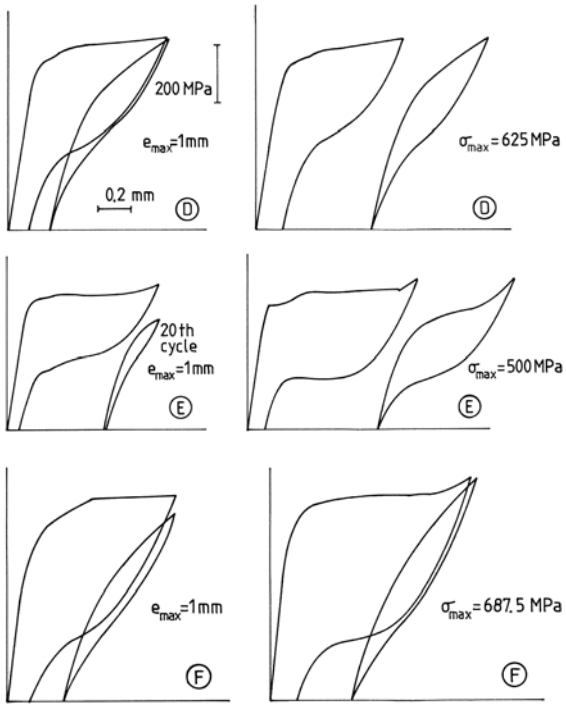

Fig.2b Stress-strain characteristics after the first and fiftieth cycles of ternary Ti-Ni-Cu alloys D, E and F

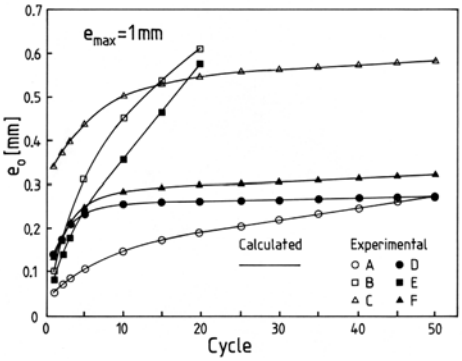

Fig.3a Residual elongation versus number of cycles, in hard cycling: experimentally ascertained point values, and curves calculated by means of equation (13)

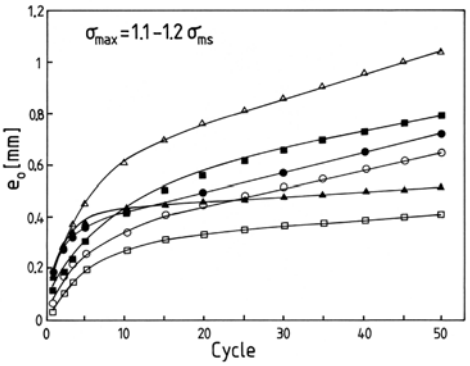

Fig.3b Residual elongation versus number of cycles, in soft cycling: experimentally ascertained point values, and curves calculated by means of equation (13)

$\sigma_{\max}$ was 1.1 to 1.2 σ_{ms}, i.e. 1.1 to 1.2 times the critical stress for martensite induction in the first cycle. The elongation measuring instrument was attached to the specimen by grips so as to detect only the true strain and not any nonsubstantial strains. In view of previous experience [4], the extension rate was held to 0.01 mm/s, which at an initial gauge length of 25 mm between grips represented a strain rate of 4.10^{-4} s^{-1}. The stress-strain diagrams recorded during the first and during the fiftieth cycles are represented for binary alloys in Fig. 2a and for the ternary alloys in Fig. 2b. The experimentally established responses of residual

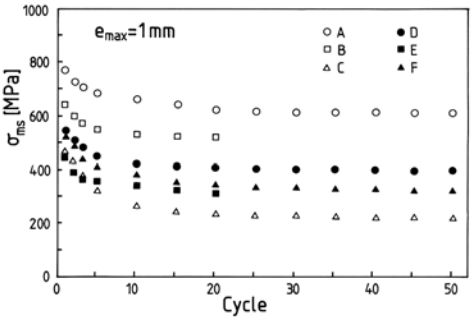

Fig.4a Experimentally established dependence of the critical stress for inducing martensite on the number of cycles in hard cycling

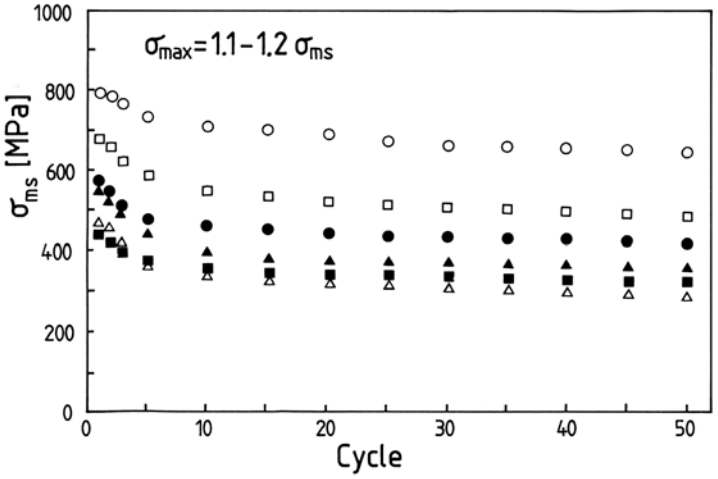

Fig.4b Experimentally established dependence of the critical stress for inducing martensite on the number of cycles in soft cycling

elongation e_0, of the critical stress σ_{ms} for martensite formation, and of hysteresis W, are plotted in Figs. 3, 4 and 5, where part *a* of every diagram applies to the hard and part *b* to the soft cycling mode.

3. Effect of cycling on residual elongation

Stress-induced martensite transformation is as a rule nucleated, as Otsuka *et al.* [5] have observed, in the middle of the specimen, i.e. in the maximum state of stress location, and then as strain insreases propagates towards the specimen edges. If we momentarily neglect the fact that the first formed martensite platelet can in the course of its motion link up with other platelets, then motions of the phase boundary between martensite platelets and the matrix induce some irreversible plastic strain of the

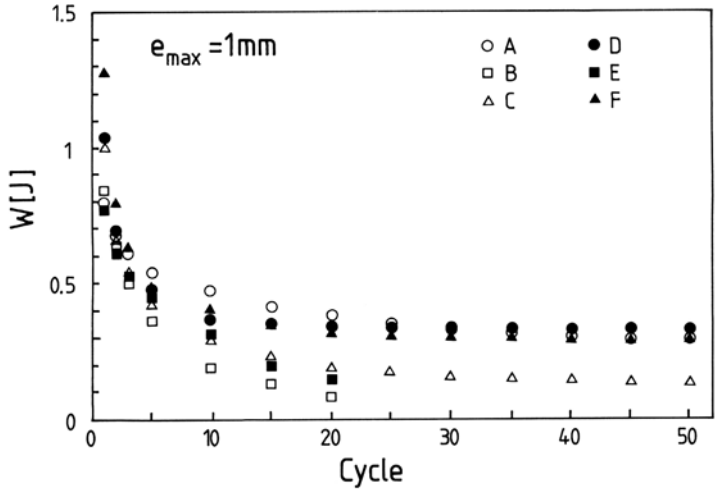

Fig.5a Experimentally established dependence of hysteresis on the number of cycles in hard cycling

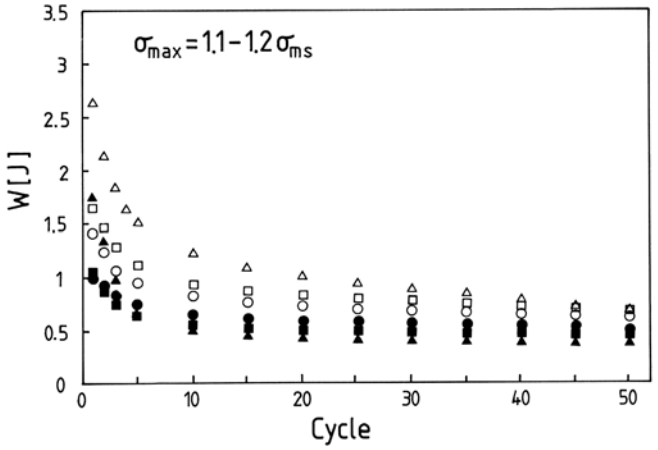

Fig.5b Experimentally established dependence of hysteresis on the number of cycles in soft cycling

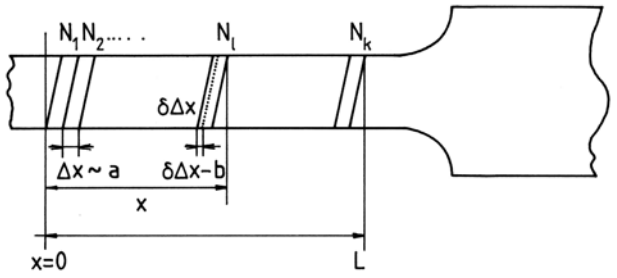

Fig.6 Scheme of plastic strain propagation in specimen

matrix, which is not recovered even after the load is relieved. On the macroscopic scale, this causes a growth of residual elongation during loading-unloading cycles. If we assume that the

rate v, at which the phase boundary that induces plastic strain propagates, is constant and not dependent on the number of cycles N, then with reference to Fig.6 this rate v can be defined as

$$v = \frac{\Delta x}{L \Delta N} \tag{1}$$

where Δx is the displacement of the plastified zone in the specimen that results from the application of ΔN cycles. Each of the specimen halves of length L is, as shown in Fig. 6, made up of k elementary volumes each Δx long, k being,

$$k = \frac{L}{\Delta x}. \tag{2}$$

It follows that the number of plastified elementary volumes is given by

$$l = \frac{x}{\Delta x} \tag{3}$$

These last two equations imply that

$$\frac{x}{L} = \frac{l}{k} \tag{4}$$

so that the plastic strain propagation rate can be inferred from equations (1) and (4) as

$$v = \frac{1}{kN}. \tag{5}$$

The increment ΔN in the number of cycles which is needed to shift the plastic zone by Δx then works out as

$$N = N_{\mathrm{i}} - N_{\mathrm{i-1}} = \frac{1}{v}\left(\frac{i}{k} - \frac{i-1}{k}\right) = \frac{l}{vk} \tag{6}$$

where i is the number of cycles after which the i-th elementary volume begins to plastify. The plastic elongation e_{0i} of this i-th elementary volume after the specimen is unloaded is the irreversible change in the length of volume i given by the differential $\delta \Delta x$. However, this elementary elongation is not what we actually detect: owing to reorientation of the dislocation structure after unloading, as well as to misalignment of the plastified element relative to the x axis of the applied stress (see Fig. 6), the elementary elongation is projected into this x axis reduced by $b = B/k$, where B is a constant dependent on the material and on the loading mode. The real logarithmic strain in the i-th element of volume will thus be

$$\varepsilon_{ip} = \ln\left(\frac{e_{0i} - b}{a}\right) \tag{7}$$

where $a = A/k$ is roughly equal to the length of the i-th elementary volume, i.e. to Δx. If we assume that this strain increases linearly with the number of cycles, then

$$\varepsilon_{ip} = \ln\left(\frac{e_{0i} - b}{a}\right) = C\left(N - N_i\right) \tag{8}$$

where $(N\text{-}N_i)$ is the total number of cycles applied during the plastic strain of the i-th elementary volume. This equation can be modified to read

$$e_{0i} = \frac{A}{k}\exp\left[C\left(N - N_i\right)\right] + \frac{B}{k}. \tag{9}$$

As $N_i = i\Delta N$, and as the total length of the specimen is $2L$, the total residual plastic strain will be governed by the number of cycles as follows:

$$e_0\left(N\right) = 2\sum_{i=1}^{l}\left\{\frac{A}{k}\exp\left[C\left(N - i\Delta N\right)\right] + \frac{B}{k}\right\}. \tag{10}$$

The sum of this expression is

$$e_0\left(N\right) = 2\frac{A}{k}\exp\left[C\left(N - \Delta N\right)\right]\frac{1 - \exp\left(-lC\Delta N\right)}{1 - \exp\left(-C\Delta N\right)} + 2l\frac{B}{k}. \tag{11}$$

For $k \to \infty$, i.e. for a very large number of elementary volumes, we can utilize equations (5) and (6) to state that

$$e_0\left(N\right) = -\frac{2vA}{C} + 2BvN + \frac{2vA}{C}\exp\left(CN\right). \tag{12}$$

This type of analytical dependence can be generalized in the following form:

$$e_0\left(N\right) = \alpha + \beta N + \gamma\exp\left(\delta N\right). \tag{13}$$

Lines calculated by means of this expression were by the least squares method superimposed on the experimental results plotted in Figs. 3a and 3b, where residual elongation is charted against the number of cycles. Table 2 presents the values of parameters α, β, γ and δ for both of the cycling modes employed.

Table 2 Numerically calculated values of parameters from eqn. (13)

Parameter	Loading mode control parameter	A	B	C	D	E	F
α[μm]	e_{max}=1mm	143	340	536	253	148	279
	σ_{max}=const.	306	289	574	344	478	417
β[μm/cyc]	e_{max}=1mm	2.54	13.60	0.88	0.39	21.10	0.90
	σ_{max}=const.	6.80	2.35	9.38	7.57	6.33	1.95
γ[μm]	e_{max}=1mm	-111	-329	-232	-172	-148	-220
	σ_{max}=const.	-285	-308	-519	-257	-404	-381
δ[cyc^{-1}]	e_{max}=1mm	-0.165	-0.254	-0.162	-0.415	-0.515	-0.383

	σ_{max}=const.	-0.213	-0.193	-0.227	-0.469	-0.137	-0.437

4. Discussion

Like previous research [1-4], the present work confirmed that the fundamental characteristics of Ti-Ni and Ti-Ni-Cu shape memory alloys in the pseudoelastic state are strongly affected by mechanical cycling and by the conditions in which it is conducted. The shape of the stress-strain diagrams for the first and fiftieth cycles in both stressing modes, as seen in Figs. 2a and 2b, indicates that hysteresis declines as the number of cycles grows. Comparison of this hysteresis versus number of cycles relationship in hard cycling, Fig. 5a, and in soft cycling, Fig. 5b, demonstrates that hysteresis drops off more rapidly in hard cycling. In hard cycling, the martensite phase transformation is incomplete and is restricted by the maximum elongation; this limitation together with the residual elongation increments in the course of cycling reduce the amount of elongation available for transformation, so that hysteresis diminishes very quickly. In soft cycling, every cycle resuls in a complete martensite transformation, so that hysteresis does not drop off as abruptly as the number of cycles increases. Higher nickel contents in both the Ti-Ni and the Ti-Ni-Cu alloys tends to reduce hysteresis; but this becomes apparent only in soft cycling, i.e. only if the martensite transformation is complete, as is evident on the right-hand sides of Figs. 2a and 2b. This lower hysteresis at higher nickel contents is attributed chiefly to the lesser transformation strain which is due to the intense resistance of the dislocation structure against movements of the new interface between the parent phase and the newly formed martensite. Yet even in the lower nickel alloys, strain hardening of the structure during cycling also severely limits the transformation strain, so that in the course of cycling the hysteresis declines quite fast.

The cyclic strain hardening mechanism also very markedly affects changes in the critical stress magnitude for martensite induction σ_{ms}, in response to cycling. This σ_{ms} stress diminishes more rapidly in lower nickel alloys such as alloy C ($Ti_{50}Ni_{50}$) or E ($Ti_{50}Ni_{40}Cu_{10}$), as is clear from Figs. 4a and 4b; this is ascribed to internal stresses set up by slip deformation in the preceding cycle. It seems probable that the internal stresses act in combination with the applied stress to induce the formation of new martensite, so that the critical stress level for inducing martensite, as measured by the applied stress, grows smaller as the number of cycles increases. However, the internal stress set up in the structure must also depend on the critical stress for slip σ_s. Given a good cyclic strain hardening capacity of the alloy, a low σ_s generally implies a greater decrease of σ_{ms} as cycling progresses. This is evident in alloy C cycled in the hard mode: by the 25th cycle σ_{ms} is down to roughly half its initial magnitude, and from then on the stress-elongation diagram remains stable. Soft cycling of the alloy C did not produce so pronounced a drop in σ_{ms}, but σ_{ms} continued to decline gradually even after larger numbers of cycles, and the stress-elongation characteristic failed to stabilize, because the hardening effect intensified as cycling proceeded. The higher nickel binary alloys A ($Ti_{49.1}Ni_{50.9}$) and B ($Ti_{49.5}Ni_{50.5}$) displayed higher σ_s values, less cyclic strain hardening and less induced internal stress, so that in the course of their cycling σ_{ms} did not drop off as quickly as it did in alloy C. The ternary alloy F ($Ti_{48.5}Ni_{41.5}Cu_{10}$), notable for its considerable cyclic dislocation hardening capacity, needed only 10 to 15 cycles for its σ_{ms} stress to stabilize. The two lower-nickel Ti-Ni-Cu alloys exhibited lower σ_s levels, a lesser strain hardening capacity, consequently lower internal stress magnitudes, and therefore their σ_{ms} stresses did not decline so profoundly in the course of cycling.

As the critical stress for slip varies with the nickel content, in the last analysis the residual elongation, or rather its response to cycling is also dependent on the Ni content and on the strain hardening capacity of the alloy. This is obvious from the first-cycle curves in Fig. 2a for e_{max} = 1 mm, where alloy A, with the highest nickel content and hence highest σ_s level, displays the least residual elongation, because in this case σ_s is smaller than σ_{ms}; cycling naturally increases this residual elongation, as is seen in Figs. 3a and 3b; but the nature of the residual elongation response depends apart from the Ni content and σ_s value also on the cycling mode. In general, a soft cycle at constant σ_{max} produces more residual elongation than a hard cycle at an e_{max} of 1 mm, which is evident from Figs. 3a and 3b. The longer or even complete martensite transformation in the tensile part of the cycle naturally causes more plastic strain.

Yet the lesser residual plastic elongation that results from hard cycling is not sufficient for the residual elongation response to stabilize. Hard cycling at e_{max} = 1 mm of alloys B ($Ti_{49.5}Ni_{50.5}$) and E ($Ti_{50}Ni_{40}Cu_{10}$) evidently involved too little elongation and too little applied stress to caused marked cyclic hardening, so that the residual elongation failed to stabilize as cycling progressed. On the other hand, soft cycling at a greater maximum elongation and hence higher stress level produced enough dislocation hardening for σ_s to rise, and residual plastic elongation did not increase as rapidly in the course of cycling as was the case in hard cycling. All this is to some extent reflected in the value of parameter α in equation (13), see Table 2. On comparison with equation (12), we can consider this a more or less constant specimen elongation, in no way dependent on the number of cycles, which is caused solely by dislocation hardening after heat treatment and the strain hardening capacity of the alloy. Table 2 shows that parameter α is much greater for soft than for hard cycling. The only exception is perhaps alloy B, where rapid hardening results in residual plastic elongation growing substantially faster in hard than in soft cycling. In alloys B and E, instability of the residual plastic elongation, as hard cycling proceeds, is reflected in a high value of parameter β, which we can regard as a cycling rate of residual elongation growth, expressed in μm/cycle. Table 2 indicates that in alloy C this rate is much greater in soft than in hard cycling at roughly the same magnitude of parameter α. This is explained by the cyclic dislocation hardening that takes place at large maximum elongations and high maximum applied stresses, and the consequent increase in the critical stress for slip. However, hardening can not raise σ_s quickly enough for this stress to exceed σ_{ms}, and than results a rapid rise of residual plastic elongation. In the hard cycling of alloy C, the low σ_s level causes severe residual elongation after unloading; much less deformation remains available for the martensite transformation; and hence the maximum applied stress level decreases; further cycling produces no further hardening; and residual elongation soon stabilizes. The outcome is a very low cyclic residual elongation rate, or parameter β.

Among the ternary alloys, alloy D has much the same residual elongation response to cycling as alloy C among the binary ones. In soft cycling, its large value of parameter β, the cyclic residual elongation rate, is due to the high maximum applied stress and the consequent hardening; but this hardening is not intense enough for σ_s to exceed σ_{ms}. In the hard cycling of this alloy, the much lower value of β is due to the restricted extent of the martensite transformation, and to the gradual lessening of the maximum applied stress as cycling proceeds; that tends to stabilize the residual elongation. In alloy F, which had the highest nickel content and hence the highest σ_s level of the investigated Ti-Ni-Cu alloys, both hard and soft cycling involved maximum elongation and maximum applied stresses large enough to produce cyclic dislocation hardening, a further rise in σ_s, and thus to stabilize the residual elongation after unloading of the specimen. This is reflected in the small magnitude of β.

Parameters γ and δ in equation (13) indicate the cyclic strain hardening capacity of the alloy: as members of the last term of that equation, they show how residual elongation diminishes as the number of cycles rises. Parameter γ represents the absolute magnitude of this reduction, as an approximation for the zero cycle, while parameter δ is the reduction magnitude for one cycle. As γ grows the cyclic hardening decreases, and this means that residual plastic elongation is not reduced so markedly. As δ grows the cyclic hardening grows too, lowering the value of the third term in equation (13), so that residual plastic elongation is reduced more intensely. In the hard cycling of the alloy B, parameter γ was small, but δ was very small too, so that cyclic hardening was only slight, and consequently residual plastic elongation remained unstable throughout the cycling. In the hard cycling of alloy E, this instability of residual plastic elongation showed up both in the high value of γ and in very low value of δ (see Table 2). In soft cycling of alloy B at approximately the same γ value as in the hard cycling, δ increased and together with the low β value tended to stabilize the residual plastic elongation. In alloy A, C and D, a transition from soft to hard cycling caused both γ and δ to increase, but α to diminish, and the residual plastic elongation, which was unstable in the soft mode, stabilized in the hard cycling. Alloy F in both cycling modes exhibited only small magnitudes of β, and γ, which at not too low values of δ reflect the stability of residual plastic elongation as the number of cycles grows.

This model of the response of residual plastic elongation to mechanical cycling does not cover the absolute magnitudes of parameters α and γ (compare equation (12) and (13)). Numerical treatment of experimental findings did reveal some differences between these two parameters, as is evident in Table 2, but only in the hard cycling of alloy C and in both the hard and soft cycling of alloy D did these relative differences exceed 20%. These differences in their absolute values express the different characters of these two parameters. While α is a measure of the residual elongation governed by dislocation hardening (and in the case of alloy A probably also dispersion hardening) effected before the testing itself commenced, parameter γ is a measure of cyclic strain hardening in the course of the testing. The model presented here does not take this difference between the two parameters into account, but it nevertheless offers an adequate explanation of the way residual plastic elongation grows with the number of cycles; a characteristic which is essential for assessing whether a given shape memory alloy in its pseudoelastic state is suitable for a given practical application. As is evident from Figs. 3a and 3b, agreement between the figures calculated by means of equation (13) and experimental results is very close indeed.

5. Conclusions

Both hard and soft cycling of Ti-Ni and Ti-Ni-Cu shape memory alloys in their pseudoelastic state has shown that the critical stress for inducing martensite σ_{ms}, and hysteresis W both decline, but residual elongation e_0 grows, as the number of elapsed cycles increases. This growth of e_0 and decline of σ_{ms} both depend on the critical stress for slip σ_s, but also on the cycling hardening capacity of the alloy. A higher σ_s, and more intense cyclic dislocation hardening promoted by greater maximum deformation and greater maximum applied stresses, in general reduce the rate at which residual elongation grows with the number of cycles, and tend to stabilize the cyclic stress-elongation diagrams. The small magnitude of σ_s in low nickel alloys, as well as pronounced cyclic strain hardening (which is supported by large residual elongations) induce greater internal stresses and a more marked decrease of σ_{ms} as cycling

progresses. The fact that hysteresis diminishes in the course of cycling is due to the restriction of transformation strain, which is caused in hard cycling by the cumulation of residual strain and in soft cycling chiefly by the increasing resistance of the dislocation structure against movements of the phase boundary. Lower nickel alloys display lesser σ_s values and more residual plastic strain, and therefore their hysteresis drops off more rapidly in hard than in soft cycling.

This model of the way residual plastic elongation varies with the number of elapsed cycles enables us to identify the three main factors that govern the magnitude of this residual elongation. One is the residual plastic elongation caused by dislocation hardening after the alloy is heat treated, as represented by parameter α. The other two are cyclic strain hardening components represented by the remaining two terms in equation (13): term βN describes how residual elongation grows with the number of cycles, parameter β being the cyclic residual elongation rate; term $\gamma \exp(\delta N)$ describes how this residual elongation is reduced, as the number of cycles increases, by the rising critical stress level for slip, in other words by cyclic dislocation hardening. This analytical dependence of residual elongation on the number of cycles has proved to yield very close agreement with experimental findings.

Acknowledgements

The presented results were obtained within the frame of solution of the research project MSM 6198910013 „Processes of preparation and properties of highly pure and structurally defined materials".

Literature

[1] Miyazaki S., Mai T.I, Igo Y., Otsuka K.: Metallurgical Transactions A 17A, 1986, pp. 115-120.
[2] Miyazaki S., Otsuka K.: ISIJ International 29, 1989, pp. 353-377.
[3] Miyazaki S.: Engineering Aspects of Shape Memory Alloys, Ed. by T.W.Duering et al., Butterworth-Heinemann Ltd., 1990, pp. 393-413.
[4] Strnadel B., Ohashi S., Ohtsuka H., Miyazaki S., Ishihara T.: Materials Science and Engineering A202, 1995, pp. 148-156.
[5] Otsuka K., Wayman C.M., Nakai K., Sakamoto H., Shimizu K.: Acta Metallurgica 24, 1976, pp. 207-226.